

ARTICLE

## Negatively-charged supported lipid bilayers regulate neuronal adhesion and outgrowth

Received 00th January 20xx,  
Accepted 00th January 20xx

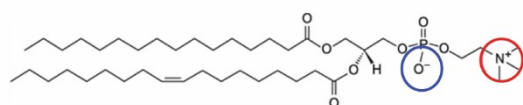
Chiara Ausilio <sup>a</sup>, Claudia Lubrano <sup>abcd</sup>, Anna Mariano <sup>a</sup>, Francesca Santoro <sup>\*acd</sup>

DOI: 10.1039/x0xx00000x

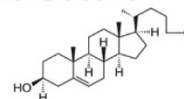
### Supporting information

Figure S1. Overview of lipid's structures.

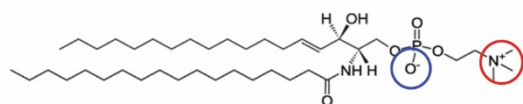
#### A. POPC



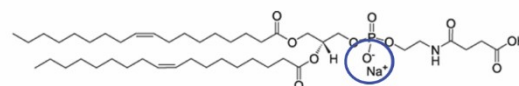
#### B. Cholesterol



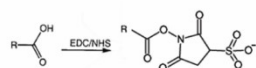
#### C. Sphingomyelin



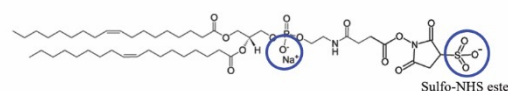
#### D. Succinyl-PE



#### E. EDC/NHS reaction



#### F. Sulfo-NHS-Succinyl-PE



Chemical structures of the lipids used for SLBs synthesis, evidencing the charged groups. The blue and red circles indicate negatively charged and positively charged groups, respectively. (A) POPC and (C) sphingomyelin are zwitterionic lipids most frequently found in the neuronal membrane.<sup>1,2</sup> (B) Cholesterol was also incorporated in SLBs. (D) Negatively charged Succinyl-PE lipid presenting an unbalanced PO<sup>3-</sup> was introduced in order to incorporate some negative charges inside SLBs. (E) An EDC/NHS reaction was used to convert the carboxylic

<sup>a</sup> Tissue Electronics, Istituto Italiano di Tecnologia, 80125 Napoli, Italy.

<sup>b</sup> Dipartimento di Chimica, Materiali e Produzione Industriale, Università di Napoli Federico II, 80125, Naples, Italy.

<sup>c</sup> Faculty of Electrical Engineering and Information Technology, RWTH Aachen, 52074, Germany.

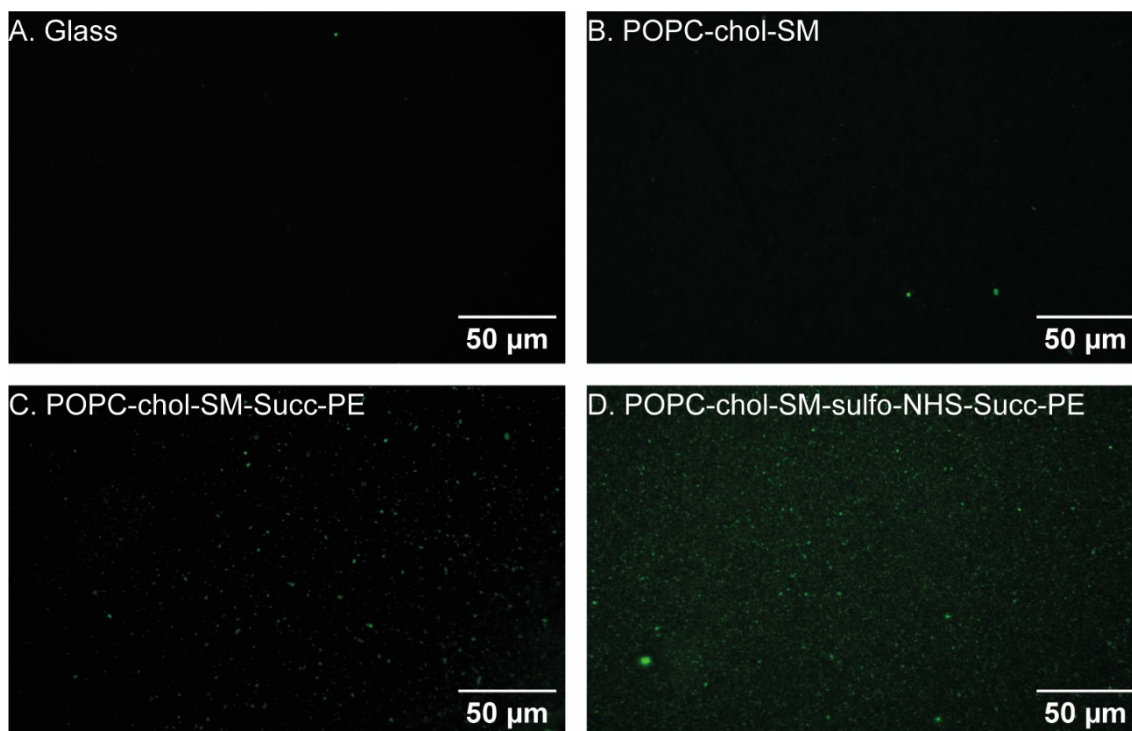
<sup>d</sup> Institute for Biological Information Processing-Bioelectronics, IBI-3, Forschungszentrum Juelich, 52428, Germany.

† Footnotes relating to the title and/or authors should appear here.

Electronic Supplementary Information (ESI) available: [details of any supplementary information available should be included here]. See DOI: 10.1039/x0xx00000x

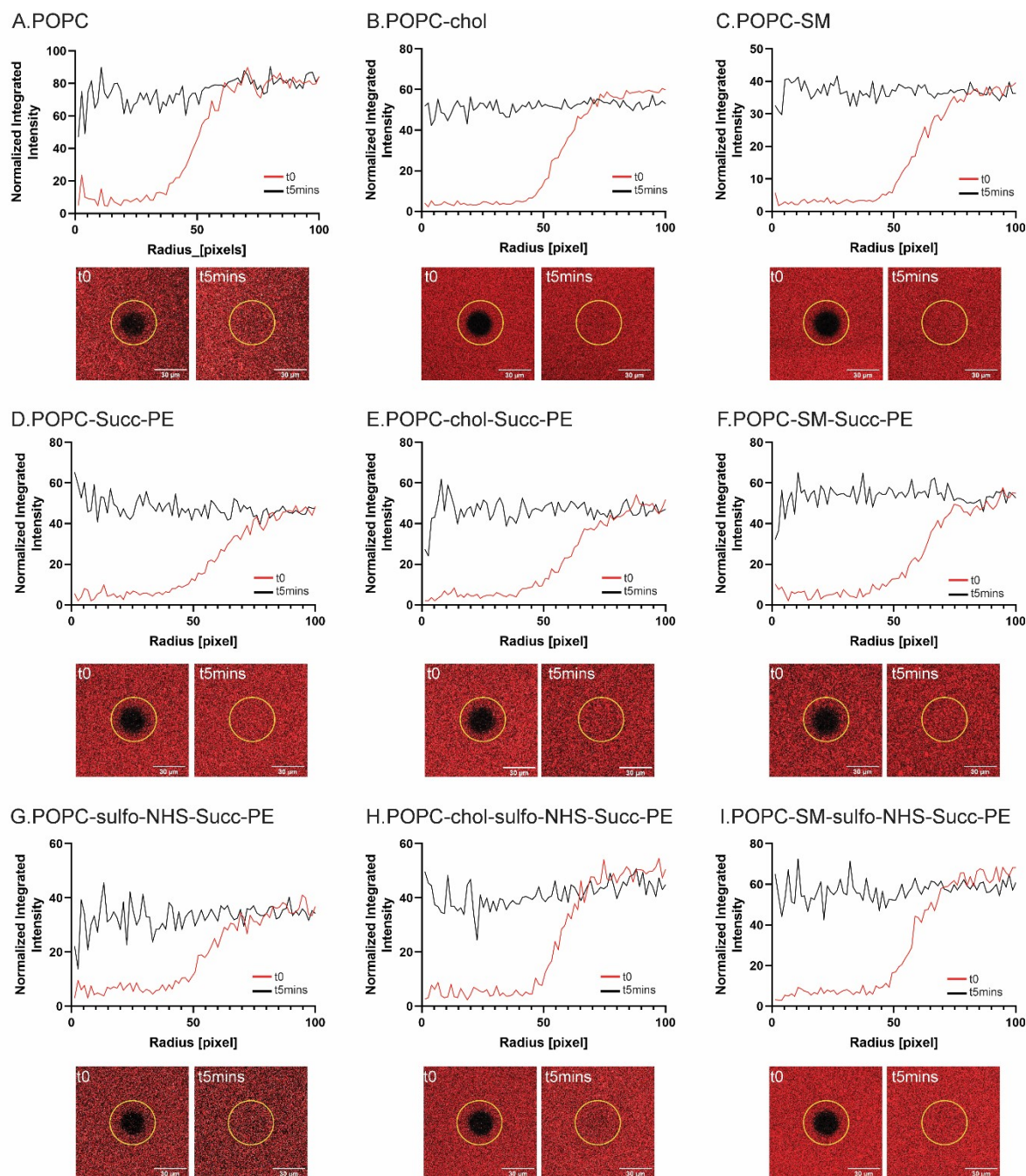
acid of Succinyl-PE lipid, to NHS-ester group.<sup>3</sup> (F) Sulfo-NHS Succinyl-PE lipid after the EDC/NHS reaction presenting unbalanced  $\text{PO}_3^-$  and  $\text{SO}_3^-$  groups.

Figure S2. SLBs surface charges.



Fluorescence images of fluorescent positively charged amine-modified latex beads (green signal) on (A) positively PLL-coated glass, (B) neutral POPC/chol/SM, (C) negatively POPC/chol/SM/Succ-PE and (D) negatively POPC/chol/SM/sulfo-NHS-Succ-PE.

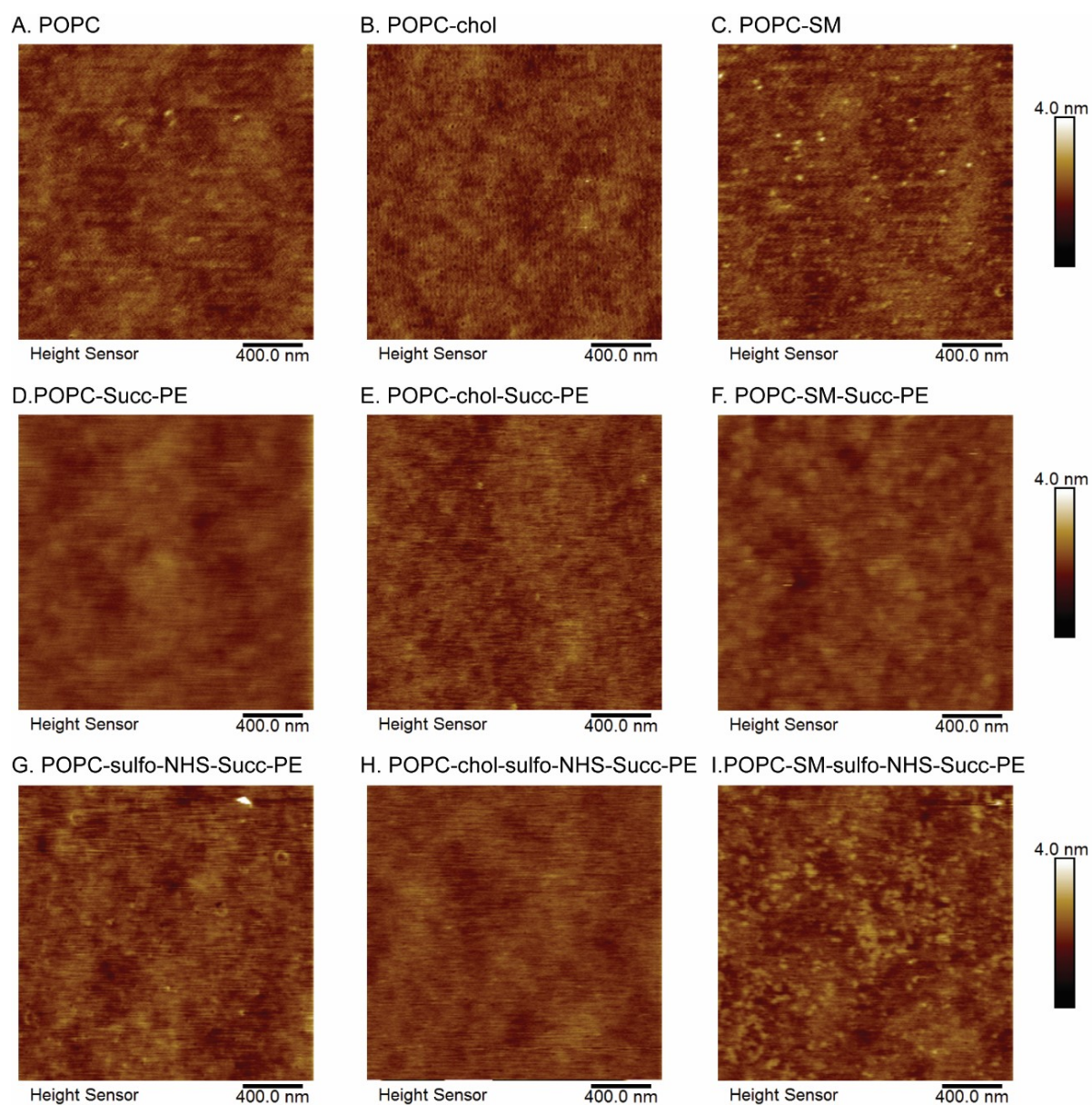
Figure S3. SLBs fluidity characterization.



Normalized fluorescence intensity profiles and FRAP snapshots of (A) POPC, (B) POPC/chol, (C) POPC/SM, (D) POPC/Succ-PE, (E) POPC/chol/Succ-PE, (F) POPC/SM/ Succ-PE, (G) POPC/sulfo-NHS-Succ-PE, (H) POPC/chol/sulfo-NHS-Succ-PE and (I) POPC/SM/sulfo-NHS-Succ-PE. The

recovery of the fluorescence intensity after photobleaching is shown at  $t = 0$  and 5 minutes. The bilayers exhibit complete fluorescence recovery after 5 minutes, confirming the correct formation of SLBs.

Figure S4. Surface morphology characterization of SLBs synthesized on glass.



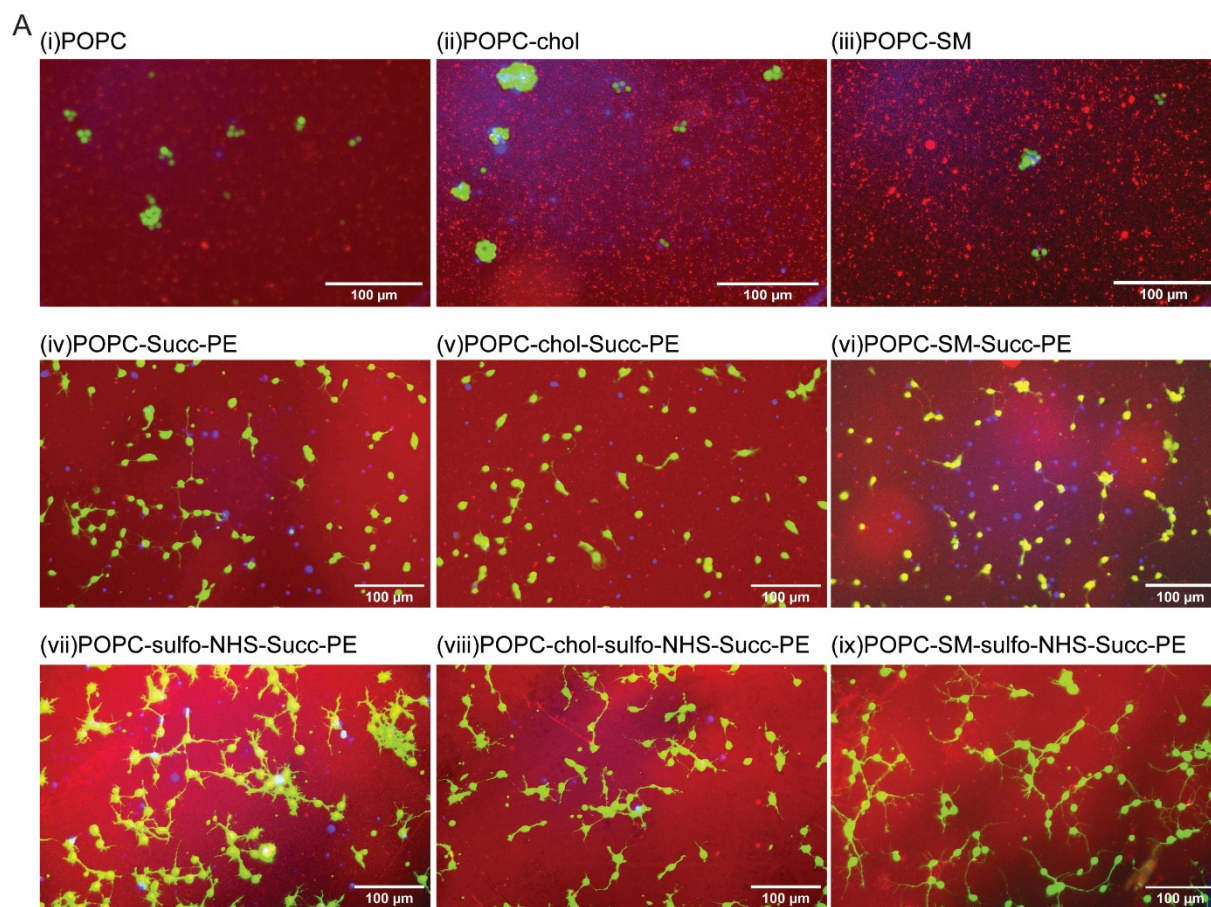
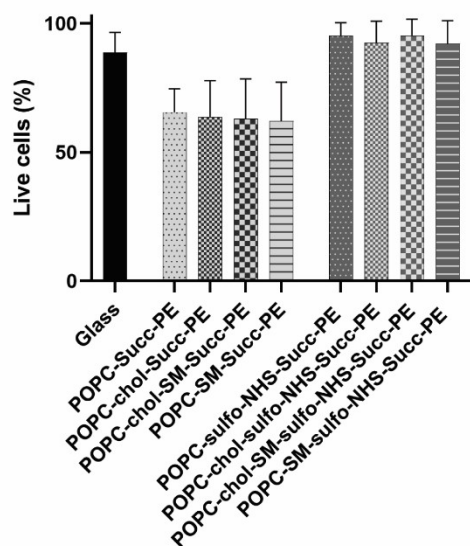
AFM images of surface morphologies of (A) POPC, (B) POPC/chol, (C) POPC/SM, (D) POPC/Succ-PE, (E) POPC/chol/ Succ-PE, (F) POPC/SM/ Succ-PE, (G) POPC/sulfo-NHS-Succ-PE, (H) POPC/chol/ sulfo-NHS-Succ-PE and (I) POPC/SM/ sulfo-NHS-Succ-PE. All lipid compositions allow the formation of homogeneous and defect-free surfaces on glass. In particular, the presence of cholesterol (B-E-H) did not cause phase separation as it intercalated between the lipids' chains.<sup>4</sup> By contrast, the incorporation of the sphingomyelin (C-I) results in the formation of granular domains, as previously observed.<sup>5</sup>

**Table S1. Diffusivity and surface roughness values of SLBs.**

Lipid mixture	Diffusivity [ $\mu\text{m}^2/\text{s}$ ]	Roughness (Ra) [ $\mu\text{m}$ ]
POPC	$1 \pm 0.2$	$134 \pm 16$
POPC-chol	$0.9 \pm 0.1$	$169 \pm 16$
POPC-chol-SM	$1.1 \pm 0.2$	$166 \pm 10$
POPC-SM	$0.9 \pm 0.1$	$160 \pm 13$
POPC-Succ-PE	$1.4 \pm 0.2$	$123 \pm 11$
POPC-chol-Succ-PE	$1.4 \pm 0.1$	$155 \pm 11$
POPC-chol-SM-Succ-PE	$1.5 \pm 0.3$	$152 \pm 39$
POPC-SM-Succ-PE	$1.5 \pm 0.1$	$120 \pm 11$
POPC-sulfo-NHS Succ-PE	$1.2 \pm 0.1$	$131 \pm 20$
POPC-chol-sulfo-NHS Succ-PE	$0.6 \pm 0.1$	$126 \pm 17$
POPC-chol-SM-sulfo-NHS Succ-PE	$0.8 \pm 0.1$	$136 \pm 22$
POPC-SM-sulfo-NHS Succ-PE	$1 \pm 0.1$	$147 \pm 23$

Diffusion coefficients and surface roughness for all the SLBs compositions are shown in Table 1 and presented as mean  $\pm$  SD ( $n = 3$ ). The presence of cholesterol decreased the diffusion coefficient depending on the lipid compositions, in agreement with previous findings.<sup>6</sup> In addition, no differences in roughness parameters have been found between the various lipids' mixtures, confirming homogeneous surface morphologies.

**Figure S5. SLBs biocompatibility.**

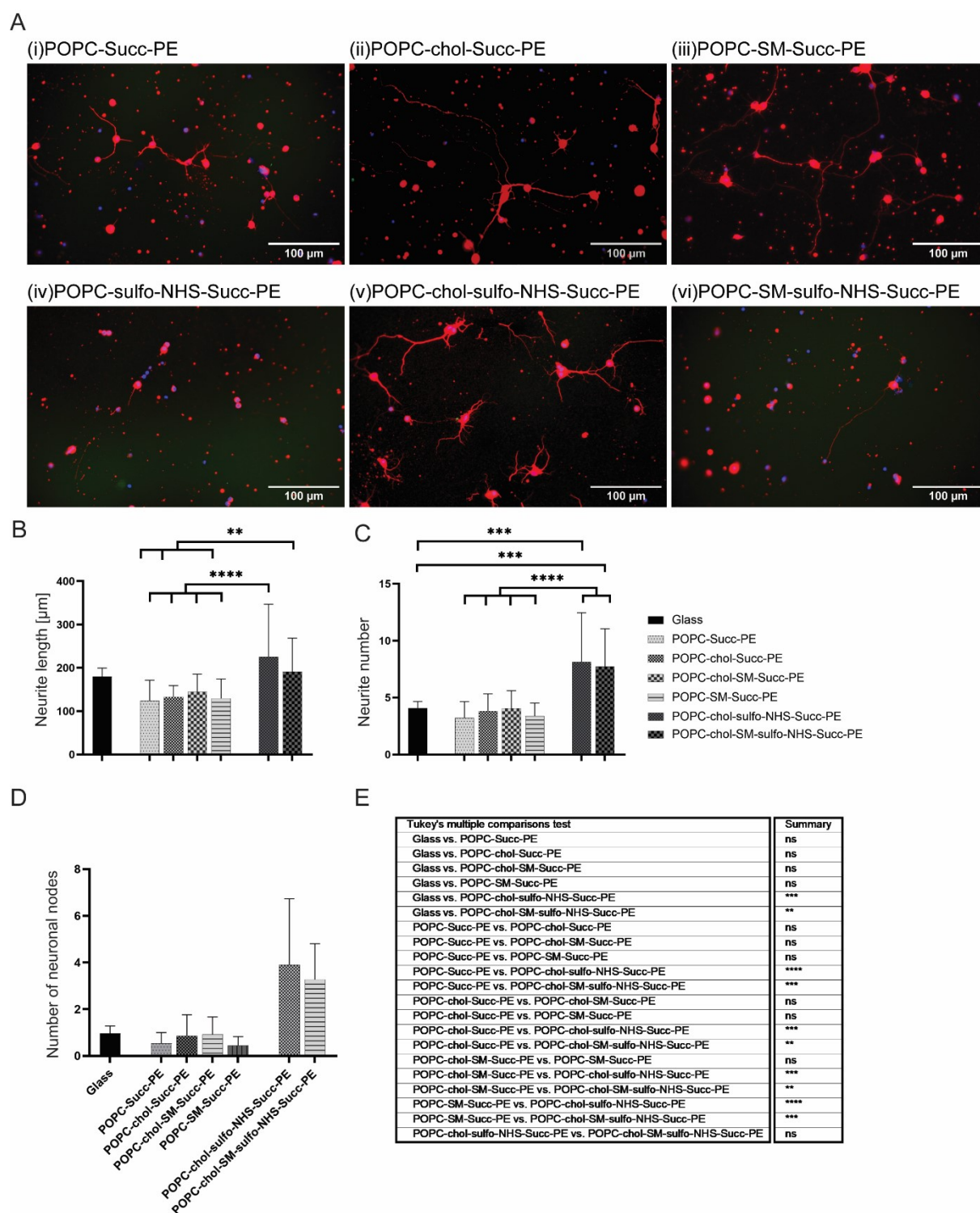
**B****C**

Tukey's multiple comparisons test	Summary
Glass vs. POPC-Succ-PE	****
Glass vs. POPC-choI-Succ-PE	****
Glass vs. POPC-choI-SM-Succ-PE	****
Glass vs. POPC-SM-Succ-PE	****
Glass vs. POPC-sulfo-NHS-Succ-PE	ns
Glass vs. POPC-choI-sulfo-NHS-Succ-PE	ns
Glass vs. POPC-choI-SM-sulfo-NHS-Succ-PE	ns
Glass vs. POPC-SM-sulfo-NHS-Succ-PE	ns
POPC-Succ-PE vs. POPC-choI-Succ-PE	ns
POPC-Succ-PE vs. POPC-choI-SM-Succ-PE	ns
POPC-Succ-PE vs. POPC-SM-Succ-PE	ns
POPC-Succ-PE vs. POPC-sulfo-NHS-Succ-PE	****
POPC-Succ-PE vs. POPC-choI-sulfo-NHS-Succ-PE	****
POPC-Succ-PE vs. POPC-choI-SM-sulfo-NHS-Succ-PE	****
POPC-Succ-PE vs. POPC-SM-sulfo-NHS-Succ-PE	****
POPC-choI-Succ-PE vs. POPC-choI-SM-Succ-PE	ns
POPC-choI-Succ-PE vs. POPC-SM-Succ-PE	ns
POPC-choI-Succ-PE vs. POPC-sulfo-NHS-Succ-PE	****
POPC-choI-Succ-PE vs. POPC-choI-sulfo-NHS-Succ-PE	****
POPC-choI-Succ-PE vs. POPC-choI-SM-sulfo-NHS-Succ-PE	****
POPC-choI-SM-Succ-PE vs. POPC-SM-Succ-PE	ns
POPC-choI-SM-Succ-PE vs. POPC-sulfo-NHS-Succ-PE	****
POPC-choI-SM-Succ-PE vs. POPC-choI-sulfo-NHS-Succ-PE	****
POPC-choI-SM-Succ-PE vs. POPC-SM-sulfo-NHS-Succ-PE	****
POPC-SM-Succ-PE vs. POPC-sulfo-NHS-Succ-PE	****
POPC-SM-Succ-PE vs. POPC-choI-sulfo-NHS-Succ-PE	****
POPC-SM-Succ-PE vs. POPC-choI-SM-sulfo-NHS-Succ-PE	****
POPC-SM-Succ-PE vs. POPC-SM-sulfo-NHS-Succ-PE	****
POPC-sulfo-NHS-Succ-PE vs. POPC-choI-sulfo-NHS-Succ-PE	ns
POPC-sulfo-NHS-Succ-PE vs. POPC-choI-SM-sulfo-NHS-Succ-PE	ns
POPC-sulfo-NHS-Succ-PE vs. POPC-SM-sulfo-NHS-Succ-PE	ns
POPC-choI-sulfo-NHS-Succ-PE vs. POPC-choI-SM-sulfo-NHS-Succ-PE	ns
POPC-choI-sulfo-NHS-Succ-PE vs. POPC-SM-sulfo-NHS-Succ-PE	ns
POPC-choI-SM-sulfo-NHS-Succ-PE vs. POPC-SM-sulfo-NHS-Succ-PE	ns

(A) Fluorescence images of primary neurons cultured on SLBs at DIV1: live cells are shown in green, dead cells in blue and SLBs in red. On neutral (i) POPC, (ii) POPC/chol and (iii) POPC/SM SLBs neuronal clusters were present, probably due to the absence of a specific surface charge.<sup>7</sup> By contrast, cells appeared well spread on the negatively charged (iv) POPC/Succ-PE, (v) POPC/chol/ Succ-PE, (vi) POPC/SM/ Succ-PE, (vii) POPC/sulfo-NHS-Succ-PE, (viii) POPC/chol/ sulfo-NHS-Succ-PE and (ix) POPC/SM/ sulfo-NHS-Succ-PE SLBs. (B) Shows the percentage of live cells (mean  $\pm$  SD, n = 3) across all compositions. (C) The complementary statistical analysis of the percentage of live cells shows a significant increase of live cells on glass and on sulfo-NHS-Succinyl-PE-containing SLBs compared to Succinyl-PE-containing SLBs, suggesting that the number of surface charges may better support the neuronal growth. (ns = not significant, \*\*\*= p < 0.0001)



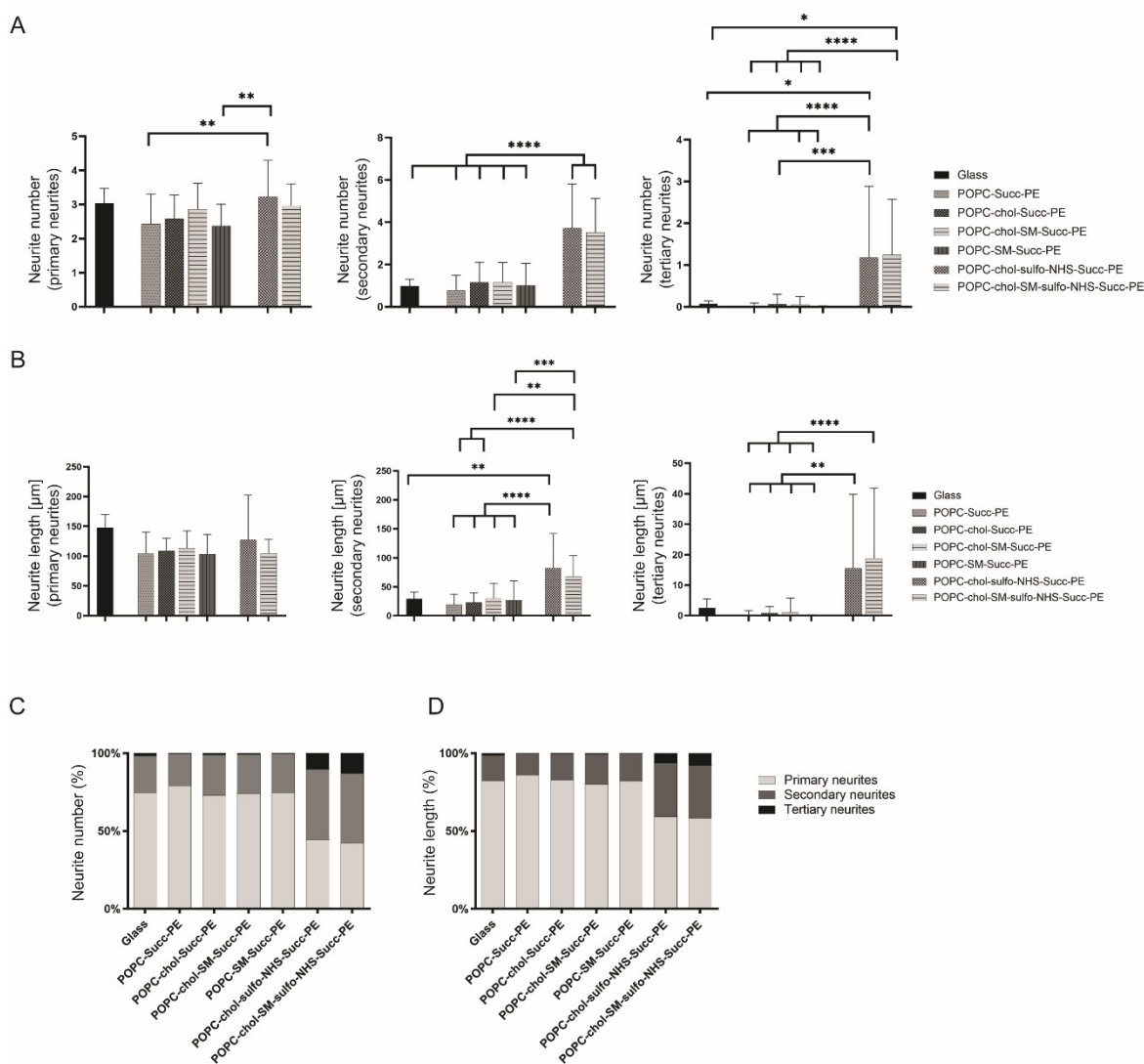
Figure S6. SLBs-mediated neurite elongation and branching.



(A) Fluorescence micrographs of primary neurons at DIV4 cultured on (i) POPC/Succ-PE, (ii) POPC/chol/ Succ-PE, (iii) POPC/SM/ Succ-PE, (iv) POPC/sulfo-NHS-Succ-PE, (v) POPC/chol/ sulfo-NHS-Succ-PE and (vi) POPC/SM/ sulfo-NHS-Succ-PE. Cells were fluorescently labelled for the nuclei (blue) and  $\beta$ -III tubulin (red). (B-C) The normalized length and number of neurites show a significant increase of both when neurons are cultured on sulfo-NHS-Succinyl-PE-containing SLBs compared to glass and Succinyl-PE-containing SLBs. (D-E) The normalized number of the nodes and the complementary statistical analysis across SLBs confirmed the increased neurites arborization on sulfo-NHS-Succinyl-PE-

containing membranes. Taken together, all these results suggest that SLBs surface charge mediates neuronal network growth, confirming that the presence of SO<sub>3</sub><sup>-</sup> groups on the SLBs surface may promote neurites sprouting. Normalized values reported as mean  $\pm$  SD (n = 3); ns= not significant, \*\* = p < 0.01, \*\*\* = p < 0.001, \*\*\*\* = p < 0.0001.

Figure S7: The effect of SLBs on neurite arborization.



(A) Number of primary, secondary and tertiary neurites. Neurons had a significantly higher number of primary, secondary and tertiary neurites on sulfo-NHS-Succinyl-PE-containing SLBs compared to all other compositions. (B) Length of primary, secondary and tertiary neurites. Secondary and tertiary neurites were longer on sulfo-NHS-Succinyl-PE-containing SLBs, compared to Succinyl-PE-containing SLBs, whereas the length of primary neurites did not change significantly. This was further confirmed by (C) the percentage of primary, secondary and tertiary neurite length on the overall length and by the (D) occurrence of primary, secondary and tertiary neurites. These results highlight how neuronal arborization and network formation is indeed mediated by surface charge and the presence of SO<sub>3</sub><sup>-</sup>. Normalized values reported as mean  $\pm$  SD (n = 3); n = 3, \* = p < 0.05, \*\* = p < 0.01, \*\*\* = p < 0.001, \*\*\*\* = p < 0.0001.

## References

1. Paoletti, L., Elena, C., Domizi, P. & Banchio, C. Role of Phosphatidylcholine during Neuronal differentiation. *IUBMB Life* n/a-n/a (2011) doi:10.1002/iub.521.
2. Hussain, G. *et al.* Role of cholesterol and sphingolipids in brain development and neurological diseases. *Lipids Health Dis* **18**, 26 (2019).
3. Huang, C.-J. *et al.* Type I Collagen-Functionalized Supported Lipid Bilayer as a Cell Culture Platform. *Biomacromolecules* **11**, 1231–1240 (2010).
4. Connell, S. D. & Smith, D. A. The atomic force microscope as a tool for studying phase separation in lipid membranes (Review). *Molecular Membrane Biology* **23**, 17–28 (2006).
5. Giocondi, M.-C., Boichot, S., Plénat, T. & Le Grimmellec, C. Structural diversity of sphingomyelin microdomains. *Ultramicroscopy* **100**, 135–143 (2004).
6. Tabaei, S. R. *et al.* Formation of Cholesterol-Rich Supported Membranes Using Solvent-Assisted Lipid Self-Assembly. *Langmuir* **30**, 13345–13352 (2014).
7. Tu, Q. *et al.* Effects of surface charges of graphene oxide on neuronal outgrowth and branching. *Analyst* **139**, 105–115 (2014).